Thermogelling of Highly Branched Poly (*N*-isopropylacrylamide)

Wei Tao, Lifeng Yan

Hefei National Laboratory for Physical Sciences at the Microscale and Department of Chemical Physics, University of Science and Technology of China, Hefei 230026, People's Republic of China

Received 22 September 2009; accepted 7 March 2010
DOI 10.1002/app.32410
Published online 14 July 2010 in Wiley InterScience (www.interscience.wiley.com).

ABSTRACT: Highly branched poly(*N*-isopropylacrylamide) (PNIPAM) has been synthesized by a reversible addition-fragmentation chain transfer (RAFT) copolymerization of NIPAM and a vinyl contained trithiocarbonate RAFT agent. ^{1}H-NMR measurements revealed that the degrees of branch (DB) are in the range of 0.032–0.105. Laser light scattering (LLS) measurements gave the hydrodynamic radii (R_h) of the polymers to be 3.6–5.7 nm with molecular weight in the range of 1.3×10^4 g/mol–2.3×10^{-4} g/mol. Highly branched PNIPAM with terminal thiol groups were obtained by aminolysis the polymers, and the product can be oxidized by air to form disulfide bonds (—S—S—) among chains and resulting in the formation of nanoparticle in aqueous solution. Interestingly, the nanoparticle in size of $R_h \sim 80$ nm showed a thermogelling behavior to form bulk hydrogel when the temperature was increased up to 25°C due to the thermo-induced association of the PNIPAM chains among the nanoparticles. © 2010 Wiley Periodicals, Inc. J Appl Polym Sci 118: 3391–3399, 2010

Key words: branched polymer; nanoparticle; thermogelling; disulfide bonds

INTRODUCTION

Branched and hyperbranched polymers have attracted much attention for their novel properties in comparison to their linear polymers, such as the large number of terminal groups, high solubility, globular or void-containing shapes, low melting point, and solution viscosities.[1–3] Recently, a huge number of works have been done for their potential application on biomedicine and catalysis.[4–6]

The syntheses of the branched or hyperbranched polymers are still an attracting topic today. The radical solution copolymerization of a vinyl monomer with a divinyl monomer is one of the simple routes. However, it usually results in the gel formation due to crosslinking even at low monomer concentration.[7] It had been reported that both free[7] and living radical copolymerization[8] were used for the synthesis of the branched and hyperbranched polymers. Among them reversible addition-fragmentation chain transfer (RAFT) radical polymerization,[9] atom transfer radical polymerization (ATRP),[10] and initiator-fragment incorporation radical copolymerization (IFIRP)[11] have been involved.

Poly(*N*-isopropylacrylamide) (PNIPAM) is a well-known water soluble polymer with low critical solution temperature (LCST) around 32°C. Recently, Rimmer et al. synthesized a highly branched PNIPAM with imidazole end groups by a RAFT route, and the polymer was used to purify histidin tagged breast cancer susceptibility protein his_6-BRCA1.[12–14] However, the physical–chemical properties of highly branched polymer have been infrequently studied.

Both branched and hyperbranched polymers have potential forms to hydrogel by physical or chemical interactions among their multi-terminal groups, and it provides a candid method to prepare novel biomaterials.[15,16] Recently, Hennink et al. showed a synthesis of hyperbranched polyglycerol hydrogel via polymerization and crosslinking, and the hydrogel has potential application in drug delivery matrices and tissue engineering as well.[17]

The thermogelling of polymer is an interesting phenomenon for biomedical application. Hu et al. reported a thermogelling behavior of PNIPAM and poly(acrylate acid) (PAA) linear copolymer. They claimed that the formation of the interpenetrating polymer network (IPN) structure of the PNIPAM and PAA is the key factor for the thermo-responding and the gelation might be achieved by the balanced force of van der Waals interaction between PNIPAM

Correspondence to: L. Yan (lfyan@ustc.edu.cn).
Contract grant sponsor: National Natural Science Foundation of China; contract grant number: 20874095.
Contract grant sponsor: National Basic Research Program of China (973); contract grant number: 2007CB210201 and 2010CB923302.
Contract grant sponsor: The Fundamental Research Funds for the Central Universities

networks and the ionic repulsion of the PAAc networks in the IPN particles.[18] Thermoresponsive physical and chemical gel constructed by crosslinking of polymer is a potential candidate for drug delivery system. Ding et al. reported a triblock linear copolymer, poly(ethylene glycol)–poly(propylene glycol)–poly(ethylene glycol) with end-capped by acryloyl groups using a biodegradable oligolactide as space which shows a thermogelling behavior.[19]

In our knowledge, there is seldom report available on thermogelling of branched/hyperbranched polymer so far.[20] The thermogelling of branched/hyperbranched polymer should have potential application as injectable materials with novel properties. Generally, they exist in liquid state at low temperature and they become gel after injecting them into the body due to the heating by the warm body.

Here, highly branched PNIPAMs were prepared by an living radical controlled copolymerization of NIPAM monomer and a vinyl contained trithiocarbonate, which works as both monomer and RAFT agent (Scheme I),[12–14] and the multi-thiols capped PNIPAMs were obtained by aminolysis of the as-prepared hyperbranched PNIPAMs, and then the products were oxidized by air in aqueous solution to form nanoparticles. The thermogelling of the nanoparticles were studied.

EXPERIMENTAL SECTION

Materials

N-Isopropylacrylamide (Acros, 99%) was recrystallized three times from hexane. Azobis(isobutyronitril) (AIBN, Shanghai First Reagent, 95%) was recrystallized from methanol. Vinylbenzyl chloride (Acros, mixture of *m*- and *p*-isomer, 96%), Ethanethiol (Acros, 99%), Zinc powder (Alfa, 99.9%). 1,4-Dithiothreitol (98%), *N*-butylamine (CP > 98.5%), Carbon disulfide (AR), and the other reagents were purchased from Sinopharm Chemical Reagent. Ultrapure water (18.2 MΩ) was produced by a Millipore System (Millipore Q).

Synthesis of the vinyl contained RAFT agent

NaOH solution (50%, 50 mmol of NaOH) was added to a mixture of 3.75 mL ethanethiol (50 mmol) and 7.5 mL of water under stirring, and 20 mL of acetone was added subsequently. Then, the solution was stirred for at least 0.5 h until it was cooled down to ambient temperature and then the solution was treated with 3.4 mL of carbon disulfide (56 mmol) to give a clear orange solution. The reaction was carried out continuously under stirring for another 0.5 h, and it was placed in an ice-bath to lower temperature less than 10°C. Then, 7.1 mL vinylbenzyl chloride (50 mmol) was added drop by drop at temperature below 15°C. Then, the reaction was carried out at ambient temperature for 24 h and was diluted with 50 mL water. After removal of the organic solvent from the solution it appeared a red oil phase and it was extracted with 50 mL of diethyl ether. Next, the solution of diethyl ether was washed by water for three times and dried with anhydrous Na_2SO_4. Then, diethyl ether was removed by distillation under vacuum, and an orange color oil of the RAFT agent was obtained. The oil was purified by silica column with petroleum ether as eluent. ^{1}H-NMR ($DCCl_3$) ppm, δ 1.35 (t, 3H, CH_3—CH_2—S—), δ 3.35 (q, 2H, CH_3—CH_2—S—), δ 4.59 (s, 2H, —Ph—CH_2—S—(C=S)—), δ 5.25 (dd, 1H, CH=CHH), δ 5.71 (dd, 1H, —CH=CHH), δ 6.67(dd, 1H, —CH=CHH), δ 7.25 (m, 4H, —C_6H_4—).

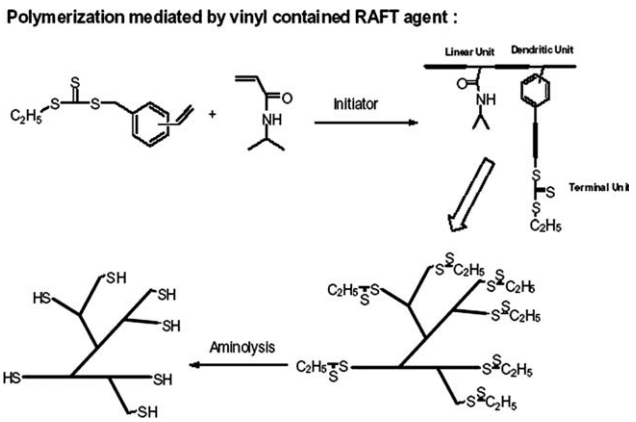

Scheme 1 Synthesis route of the highly branched PNIPAM.

Polymerization for the highly branched poly (*N*-isopropylacrylamide)

The synthesis of the highly branched PNIPAM was according to a similar method as reported in Ref. [12]. In brief, the RAFT agent, *N*-isopropylacrylamide and AIBN were dissolved in 10 mL dioxane, the solution was bubbled with N_2 for 40 min and was put into a 70°C oil-bath subsequently. After reacting under N_2 atmosphere for 15 h, the solution was cooled down by ice-water to quench the reaction and then it was poured into10-fold diethyl ether. The product was collected by filtration and dried in vacuum.

Aminolysis of the RAFT end groups of the branched polymer

The as-prepared branched PNIPAM was dissolved in 10 mL THF, and the solution was bubbled with N_2 for 30 min. Then, *N*-butylamine was added in a relation of 20 : 1 respect to the RAFT end groups present in polymer. After the reaction was carried out under N_2 atmosphere for 12 h, the solution was

poured into 150 mL diethyl ether, and the produced white precipitate was collected by filtration and dried under vacuum.

Nanoparticle formed by the multi-thiols capped branched PNIPAM

Multi-thiols capped highly branched PNIPAM was mixed with 0.2 mL water in a vial, and then it was placed in refrigerator (4°C) keeping the vial open to air for 5 days. The concentrations of the polymer were controlled by adding different amount of water. Nanoparticles were formed at low concentration under continuous oxidation by air. The nanoparticle powder can be obtained by freeze drying the relative aqueous solution. To confirm the linkage is disulfide bonds, the nanoparticles were treated with dithiothreitol (DTT) and Zn powder to observe whether they were damaged or not.

Thermogelling of the nanoparticles

The nanoparticles take a solution-to-gel transition on increasing temperature. The relationship between the gelling temperature and the concentration of the solutions was obtained as follows: a given amount of nanoparticles were dissolved in different amount of water, then the solution was kept at 10°C for 30 min and it turns to a clear solution. Then, the solution was heated by a regulated water bath to control the temperature increase at the speed of 1°C/10 min, and tipping the vial 30° during heating and if the surface of the system did not change in 1 min, the corresponding temperature was recorded as the gel temperature.[21]

Characterization of the polymer

Gel permeating chromatography

Molecular weight and its distribution (M_w/M_n) were determined on Waters Gel Permeation chromatography (GPC) (Waters, Milvord, MA). Polystyrenes as the calibration standard and tetrahydrofuran (THF) as the eluent with a flow rate of 1.0 mL/min.

^{1}H-NMR spectrum

^{1}H-NMR spectra were measured on a Bruker spectrometer (Avance 300, 300 MHz, Bremen, Germany) with $CDCl_3$ or D_2O as solvent.

Laser light scattering

A commercial spectrometer (ALV/DLS/SLS-5022F, Siemensstraße, Germany) equipped with multi-τ digital time correlation (ALV5000) and a cylindrical 22 mW UNIPHASE He–Ne laser ($\lambda_0 = 632$ nm) as the light source was used.

In static LLS, the weight-average molar mass (M_w) of particles can be obtained in a dilute solution from the angular dependence of the excess absolute scattering intensity or Rayleigh ratio $R_{vv}(q)$ by Zimm plot based on the following equation,

$$\left(\frac{KC}{R_{vv}(q)}\right)_{c\to 0} \approx \frac{1}{M_w}\left(1+\frac{1}{3}\langle R_g^2\rangle q^2\right)(q\langle R_g^2\rangle^{1/2} < 1) \quad (1)$$

where $K = 4\pi^2 n^2 (dn/dC)^2/(N_A\lambda_0^4)$ and $q = (4\pi n/\lambda_0)$ sin (θ/2) with N_A, dn/dC, and n being the Avogadro number, the specific refractive index increment, and the solvent refractive index, respectively. A_2 is the second virial coefficient.

For dynamic light scattering (DLS), the intensity–intensity time correlation function $G^{(2)}(t,q)$ was measured to determine the line-width distribution $G(\Gamma)$. For diffusive relaxation, Γ is related to the translational diffusion coefficient (D) of the scattering object (polymer chain or colloid particle) in dilute solution or dispersion by $D = (\langle\Gamma\rangle/q^2)_{C\to 0,q\to 0}$ and further to hydrodynamic radius (R_h) from the Stokes–Einstein equation: $R_h = k_B T/(6\pi\eta D)$, where η, k_B, and T are the solvent viscosity, the Boltzmann constant, and the absolute temperature, respectively. Hydrodynamic radius distribution $f(R_h)$ was calculated from the Laplace inversion of a corresponding measured $G^{(2)}(t,q)$ using the CONTIN program.[22,23] All dynamic LLS measurements were conducted at a small scattering angle (θ) of 15°.

Atomic force microscopy

AFM images were captured in the tapping mode by a NanoScope IIIa MultiMode SPM (Digital Instruments, Santa Barbara, CA) at 20°C. Silicon tip (model TESP, Nanoprobes, Digital Instruments) with cantilever length of 125 μm and resonant frequency of about 300 kHz was used. The scan rates were in between 0.5 and 1.0 Hz. Height and phase signal were recorded simultaneously. The 512 × 512 point images were recorded and analyzed by using the AFM software, WSxM 4.0 (Nanotec Electronic S. L.) and Photoshop 5.0.

US–DSC measurements

US-DSC measurements were carried on a VP DSC from MicroCal (Piscataway, NJ). The volume of the sample cell was 0.509 mL. The reference cell was filled with deionized water. Hyperbranched PNIPAM solution with a concentration of 1 mg/mL was degassed at 25°C for half an hour. The solution was equilibrated at 5°C for 2 h before the heating process. The phase transition temperature (T_p) was taken as that corresponding to the maximum specific heat capacity (C_p) during the transition. The

TABLE I
Characteristic of Branched Polymers

Polymer	DB	R_h (nm)	$M_{n\mathrm{GPC}}$ (g/mol) × 10^3	$M_{n\mathrm{SLS}}$ (g/mol) × 10^3	PDI
HP50	0.032	5.7	6.82	22	1.8
HP20	0.063	3.7	5.12	13	1.61
HP10	0.105	3.6	4.86	23	1.40

enthalpy change (ΔH) during the transition was calculated from the area under each peak.

RESULTS AND DISCUSSION

Here, three samples with different ratios of the RAFT agent, NIPAM, and AIBN were synthesized, which were labeled as HP50, HP20, and HP10, respectively. The numbers denote the molar ratios of NIPAM to the RAFT agent while the initiator is always 1/5 of the RAFT agent. Molecular weights of the highly branched polymers were measured by Gel Permeating Chromatography (GPC) and Static Light Scattering (SLS), and the results were shown in Table I. Clearly, the apparent molecular weights of the polymers determined by GPC are much smaller than the values determined by SLS, which gave the absolute molecular weight of the branching polymer.[24] Comparing with the GPC result, it seems that the M_{ns} measured by SLS have no linear relationship with the ratio of monomer to RAFT agent, indicates the complex of the polymerization. As the increasing of the ratio should increase the length of single chain and decrease the branched degree, and vice versa, so it is possible to get a high $M_{n\mathrm{SLS}}$ when the $M_{n\mathrm{GPC}}$ is small and the detail should be studied next. The results also supported the formation of the branched polymers. The structure of the polymer was determined by ^{1}H-NMR measurement. Figure 1 shows the ^{1}H-NMR spectrum measured in $CDCl_3$ of the RAFT agent, and the branched PNIPAM of HP20 before and after aminolysis. The spectrum of the branched PNIPAM can be divided into three regions: In 7.25 ppm to 5.2 ppm region, they are assigned to the chemical shift of protons of phenyls in RAFT agent and acylamide in NIPAM. The three peaks in the region of 5.0 ppm to 3.05 ppm are contributed to —*H*C(CONHC$_3$H$_7$)—S—(C=S)—,

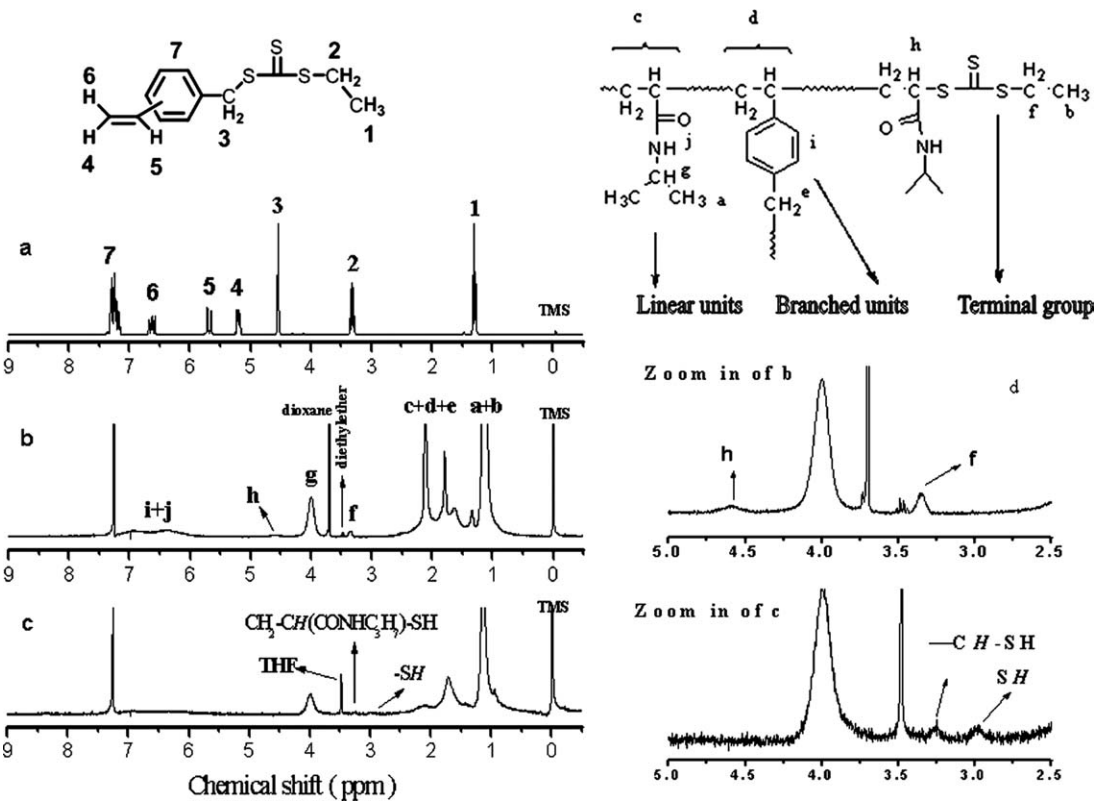

Figure 1 ^{1}H-NMR spectrum of (a) RAFT agent; (b) the highly branched PNIPAM HP20 before aminolysis; (c) the highly branched PNIPAM HP20 after aminolysis; and (d) the zoom-in of the spectrum of (b) and (c) in range from 2.5 to 5 ppm. The solvent is $CDCl_3$.

4.55 ppm; CONH—C*H*$(CH_3)_2$, 4.0 ppm; and CH_3—CH_2—S—(C=S)—, 3.32 ppm. The region from 2.9 ppm to 0.5 ppm is contributed to the protons of backbone, methyl of RAFT agent, and methyl of isopropyl. The degree of branching (DB) values are calculated according to equation[22,23] and showed in Table I:

$$\frac{\sum D + \sum T}{\sum D + \sum T + \sum L}$$

where D, T, and L denote dentritic unit, terminal unit, and linear unit, respectively, $\sum T = A_f/2$, $\sum L = A_g$, $\sum D = (A_{i+j} - A_g)/4$, A_f, A_g, and A_{i+j} denote the areas of peaks f, g, and $i+j$ labeled on ^{1}H-NMR spectra [Fig. 1(b)].

After aminolysis, the trithiolcarbonate end groups in the branched polymer were changed to the thiol groups and in the ^{1}H-NMR spectrum [Fig. 1(c,d)] there appeared two peaks at 3.0 ppm and 3.25 ppm, which attributed to the —S*H* and —CH_2—C*H*$(CONHC_3H_7)$—SH protons. The peak at 3.32 ppm for CH_3—CH_2—S—(C=S)— proton was disappeared, indicating the aminolysis of the trithiolcarbonate.

The phase transitions of the branched PNIPAM capped with trithiolcarbonate terminal groups (a) and thiol terminal groups (b) in water are studied by a microcalorimeter, as shown in Figure 2. Comparing with the temperature of phase transition (T_p) of traditional linear PNIPAM which is about 32°C,[22,23] the T_p values of the highly branched polymers HP20 is lower. This result indicates that the hydrophobic groups (trithiolcarbonate terminal units and phenyl branching units) are randomly distributed in the polymers[22,23] and the enhancement of T_p (about 10°C) of the aminolysized polymer could be rationalized considering the enhance hydrophilicity of thiol end-capped branched polymers.[25] Similar results were found for HP50. For HP10, the solubility is low and it is difficult to measure its T_p. However, it shows a huge increasing of its hydrophilicity after amninolysis and the T_p is about 16°C. The areas of curves represent the enthalpies of phase transition, and the value for the thiol end-capped polymer is much smaller than the one before aminolysis. Xia et al. reported that the hydrophilic end groups of linear PNIPAM with molecular weight smaller than 5000 Da made a sudden decrease in enthalpy of phase transition to the corresponding PNIPAM capped with hydrophobic groups, and they suggested that hydrophobic end groups may help the de-solvation of the polymers above the cloud point, whereas hydrophilic end groups may interfere with it.[26] Therefore, the big decrease in enthalpy observed in this experiment might be due to the branched

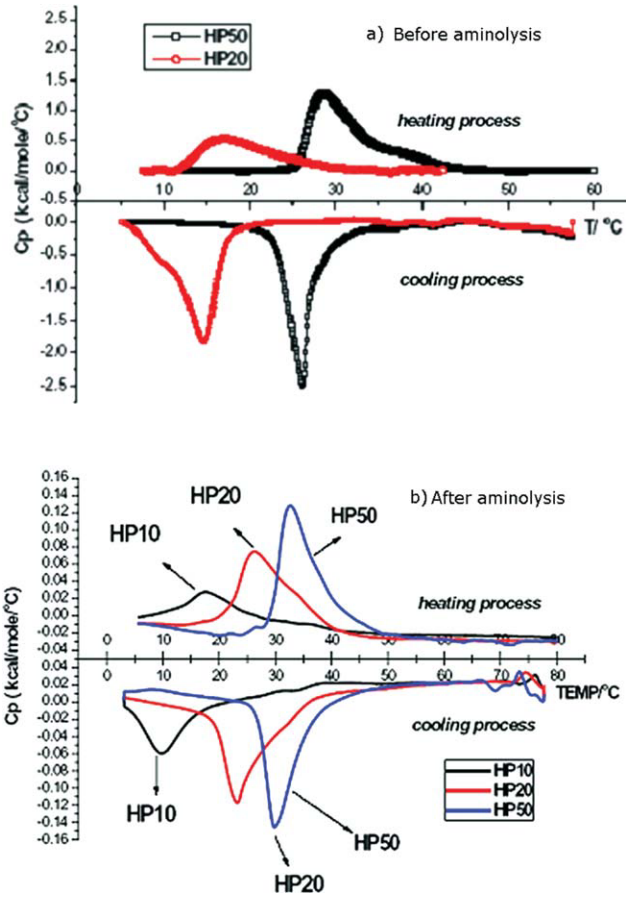

Figure 2 Temperature dependence of the specific heat capacity (C_p) of highly branched PNIPAMs in water with the concentration of 1 mg/mL (the ratio of solute to solution). (a) Highly branched PNIPAM before aminolysis; (b) highly branched PNIPAM after aminolysis. [Color figure can be viewed in the online issue, which is available at www.interscience.wiley.com.]

structure of the polymer which owns shorter linear chains, and the detail reason is still under investigation.

Thiol groups (—SH), which can conveniently be obtained by aminolysis of the RAFT agent terminal groups in a polymer,[27] are able to form disulfide bonds (—S—S—) spontaneously in a mild oxidation conditions such as exposing it to air, and can be regenerated either by Zn powder, DTT, or glutathione as reducing reducing agents.[28] In sealed condition, addition of water to the as-prepared thiol end-capped highly branched PNIPAM HP20 powder did not make clean homogeneous solution directly. First, it soaked water and formed a gel-like state. Then, addition of more water into the gel-like state brought clear solution after 2 days under seal. The solution showed a lower critical solution temperature (LCST) about 26.4°C, and it became white and turbid at 30°C, as shown in Figure 3.

The unique characteristics of disulfide bond are of it's reversibility and relative stability in plasma

Figure 3 The snapshot of the highly branched PNIPAN HP20 after aminolysis without oxidation in aqueous solution at 20°C (a) and 36°C (b). The concentration of polymer in water is 25 wt %. [Color figure can be viewed in the online issue, which is available at www.interscience.wiley.com.]

which make it attractive in designing drug-delivery systems[29] and molecular recognition materials.[30] So, some aggregative structures should be expected on exposing the solution-to-air. Figure 4(a) shows the dynamic light scattering (DLS) results of the branched PNIPAMs before and after aminolysis at different concentrations. Before aminolysis, the hydrodynamic radii of the highly branched polymer HP20 is R_h = 3.7 nm, and no big aggregates appeared even exposing the solution-to-air. However, it showed different behavior after aminolysis due to the potential S—S bonds formation of the terminal thiol groups. As shown in Figure 4(a), when the solution was exposed to air after aminolysis, it results in the formation of big aggregates, and the R_h of the particles are 34.6 nm and 79.5 nm for the concentration of 1.67 wt % and 5 wt %, respectively. The distributions of the formed nanoparticles are narrow, and the particle size can be controlled by tuning the concentration of the solution and oxidation condition. The nanoparticles were stable due to the disulfide bonds, and it may be broken by a reductant. To break the disulfide bonds, 10 mg of DTT was added into the nanoparticle system and was kept for 5 days at room temperature. As shown in Figure 4(b), the DLS result reveals that the size of the particles decreases and the distribution of R_h becomes wide with a peak at R_h = 20 nm. This result confirms that the connections among the thiol end-capped branched PNIPAM are the disulfide bonds.

A novel thermogelling behavior of the highly branched PNIPAM HP20 nanoparticle was observed in this study. The nanoparticles in size of 79.5 nm (R_h) were dispersed into aqueous solution, and then it was heated slowly. Figure 5 shows its thermogelling behavior: at 4°C the nanoparticles were well dispersed in aqueous medium [Fig. 5(a)] and upon increasing temperature up to 25°C it turns into gel

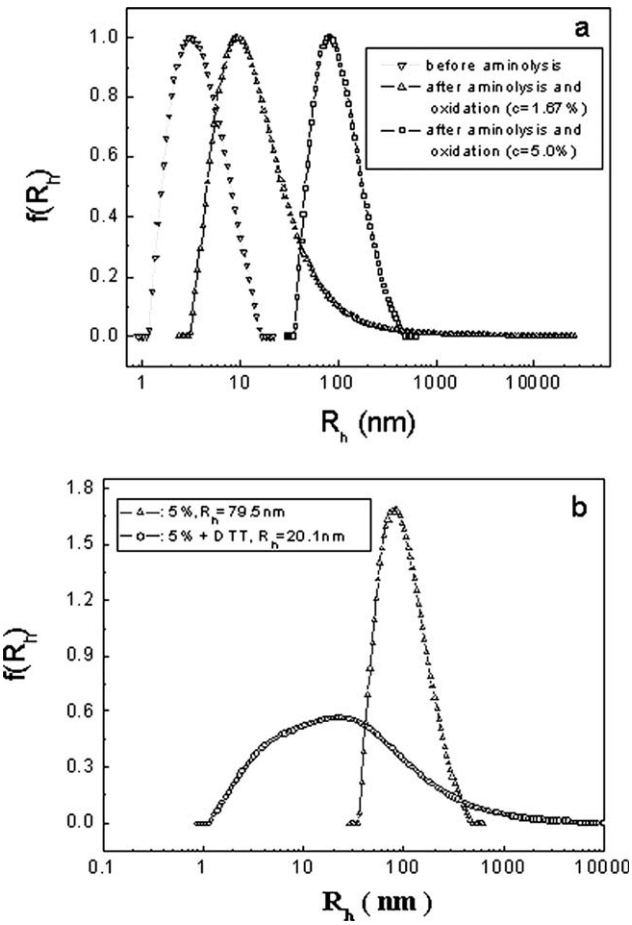

Figure 4 The hydrodynamic radii R_h and their distribution $f(R_h)$ of the highly branched PNIPAM HP20 solutions measured by DLS at various concentrations. (a) The branched polymer before aminolysis and after aminolysis plus oxidation by air at different concentrations (1.67% and 5%); (b) the size and distribution of the formed nanoparticles and the damaged nanoparticles after adding of 10 mg DTT at room temperature for 5 days.

form [Fig. 5(b)] and the gel contained excess of water. When temperature was further increased up to 35°C, water was extruded out from the gel [Fig.

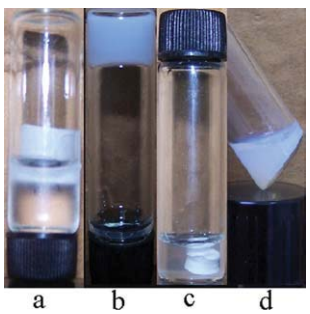

Figure 5 Snapshot of the formed nanoparticle solution in water of the highly branched PNIPAM HP20 at concentration of 5% at 4°C (a), at 25°C for 1 h (b), at 35°C for 3 h (c), and after adding 10 mg of DTT into it at 35°C (d). [Color figure can be viewed in the online issue, which is available at www.interscience.wiley.com.]

5(c)]. This thermogelling process is reversible and it could be dissolved into water by decreasing temperature. The mechanism of the thermosensitive gelation is believed to be due to the stacking of the nanoparticles along with hydrophobic association of the PNIPAM chains. The formed bulk gel is a network of nanoparticles and the nanoparticle works as the building block of the gel. Further investigations are needed to uncover the detailed mechanism of this thermogeling process. Interestingly, this thermosensitive hydrogel could also be decomposed by adding DTT into it [Fig. 5(d)] indicates that the stability of the nanoparticle is a key factor for the formation of bulk gel. Upon addition of DTT it should disrupt the nanoparticle by breaking the disulfide bonds and make the building block to disappear. No gel formation was observed when the nanoparticles of 11.3 nm of R_h are used as the building block for gel formation and the heating of the system could not turn the solution into gel form even at higher concentration. This result indicates that a critical size of the nanoparticle is essential for the said thermogelling process and this critical value of R_h should lie between 11.3 nm and 34.6 nm. When the R_h of the nanoparticles reaches up to the critical size, the thermogelling process could occur in a higher range of concentrations. Hence, there is an existence of critical gelation concentration (CGC) for particular size of nanoparticles. The CGC of the nanoparticles of HP20 with $R_h = 79.5$ nm is about 0.012 g/mL, and below this concnetration the nanoparticles precipitate on increasing temperature. The nanoparticle with R_h of 34.6 nm was also found to show a thermogelling at 22.8°C at concentration of 5 wt % and below this concentration the nanoparticles should be precipitated. So, the phase behavior of the nanoparticles strongly depended on its size and concentration.

Figure 6 shows the phase diagram of the nanogel solution with $R_h = 79.5$ nm dispersed in aqueous solution at different concentration with changing of temperature. There exist four regions: Region I is in transparent solution, Region II corresponds to turbid solution, Region III is in bulk gel, and Region IV is in precipitation. At low temperature, the nanogel can be well dissolved in water, and increasing temperature should result in the appearance of turbid solution at first, and then the formation of bulk gel. The critical gelation concentration (CGC) of the nanogel of HP20 is about 0.012 g/mL, and below that there appears precipitate with increasing temperature. The nanogel with R_h of 34.6 nm was also found a thermogelling at 22.8°C at concentration of 5 wt %, and more water would lead it entering into the Region IV. So, the phase's behavior of the nanogels strongly depends on its size.

This kind of hydrogel may have potential application in biomaterials for its thermogelling behavior.

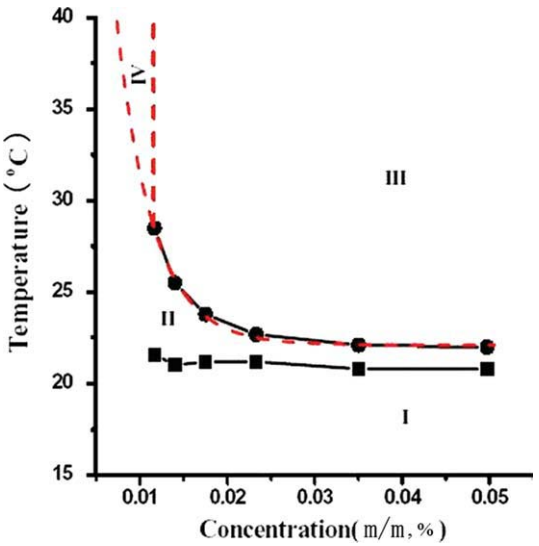

Figure 6 Phase diagram of nanogel (Sample 4) in water with concentration below 0.07 g/mL. There exist four regions: (I) transparent solution; (II) turbid solution; (III) hydrogel; (IV) precipitate. [Color figure can be viewed in the online issue, which is available at www.interscience.wiley.com.]

At low temperature, the solution is stable and can safely be added with drug to form a homogeneous solution, and then the solution could be injected into body. After that it could form hydrogel including drugs therein due to the thermogelling at body temperature and the drugs could be released slowly to the body. The prepared nanoparticle of the highly branched polymer is also a candidate as carrier to delivery drugs into cell, and its disulfide bonds property makes it possible to be decomposed inside cell due to the presence of glutathione.

The change of the morphology of the nanoparticles was also investigated by atomic force microscope (AFM). The cold aqueous solution of the nanoparticles in size of 79.5 nm (Sample A) and 34.6 nm (Sample B) were deposited directly onto the surface of freshly cleaved mica and were dried at 20°C, and then the samples were measured by AFM. Figure 7(a) shows the typical AFM image of Sample B where the appearance huge numbers of small spheres were observed and they overlap to each other. The size of the sphere is about 60 nm in diameter [Fig. 7(b)] and it is very close to that obtained from DLS study. Similarly, Figure 7(c) shows the typical AFM height image of Sample A. The size of the nanoparticle is about 120 nm and it is also consistence to the DLS results. The thermogelling process of the nanoparticles is also studied by means of AFM. Samples were prepared by dropwise deposition of 20 μL cold aqueous solution (4°C) of the polymer of Sample A or Sample B on freshly cleaved mica and then was dried at 45°C. To avoid the effect of solvent evaporation rate on the aggregation of the

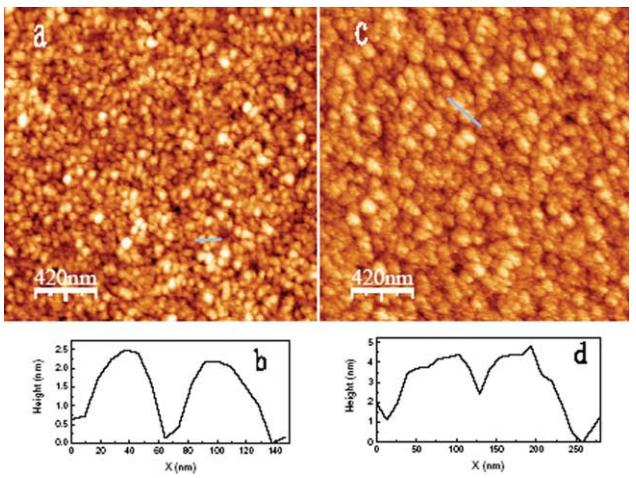

Figure 7 AFM height images of the formed nanoparticle of highly branched PNIPAM HP20 after aminolysis at concentration of 1.67% (a) and 5% (c) in water. The samples were prepared by depositing its solution onto the freshly cleaved mica at low temperature under spin-coating at 2500 rpm for 30 s, respectively. Both the images (b) and (d) are the section line analysis of the particles indicated in the figures (a) and (c). [Color figure can be viewed in the online issue, which is available at www.interscience.wiley.com.]

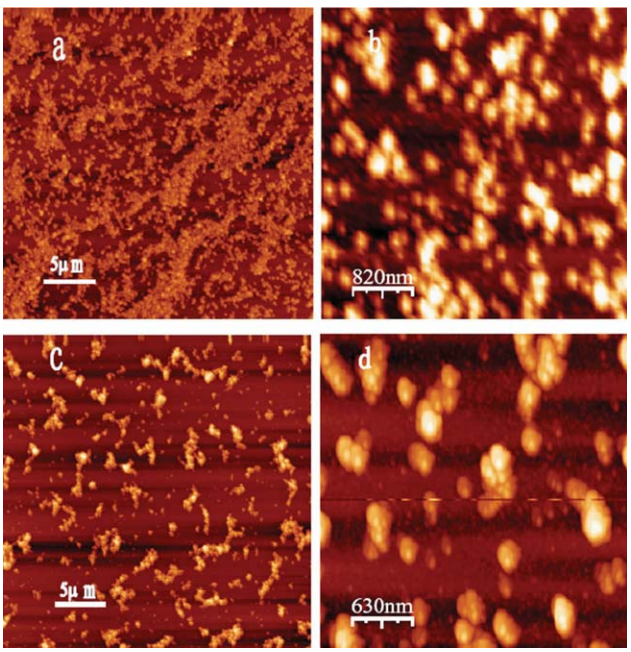

Figure 8 AFM images of the thermogelling aggregates of the highly branched PNIPAM HP20 nanoparticles on the surface of fresh cleaved mica by dropwise depositing 20 μL of its 1.67 wt % aqueous solution (4°C) and then dried at 45°C (a and b) or 20 μL of its 5.0 wt % aqueous solution (4°C) and then dried at 45°C (c and d). [Color figure can be viewed in the online issue, which is available at www.interscience.wiley.com.]

branched polymer, samples were also prepared by spinning at 2500 rpm for 30 s after placing a drop of solution on newly cleaved mica at 45°C. Figure 8 shows the typical AFM images of the sample prepared by drop deposition. When the concentration is low, they form some weakly connected structure while there formed fractal aggregates at higher concentration of polymer. The fractal aggregates is believed to be an antetype of the hydrogel.

The branched PNIPAM with thiol terminal groups has potential to form hydrophobic disulfide bonds under air oxidation and form nanoparticle at low concentration. Attend by the phenyl branching units in the polymer, the branched PNIPAM has tendency to make a self-association to decrease surface energy, while the hydrophilic PNIPAM chains has tendency to keep the particles apart from each other to combine more water. When temperature was increased, the hydrophilicity of PNIPAM chains was reduced with the collapse of the nanoparticle and resulting in the formation of bigger clusters (Scheme II). The gradual extension of hydrophobic regions at higher temperature may be the reason for the thermogel to extrude water at 35°C. The hypothesis may also be supported by the ^{1}H-NMR of the nanoparticle in D_2O (Fig. 9) and the profile of the peaks in high magnetic fields became as simple as a homopolymerized PNIPAM. The observed three separated peaks are assigned to CONH—CH(CH_3)$_2$, —CH_2—CH—, and —CH_2—CH—, respectively, and the ratio of the areas is 6:2:1. The peaks for phenyl are not observed in the NMR spectra recorded in $DCCl_3$. This result indicates that the regions of the hydrophobic groups are in a

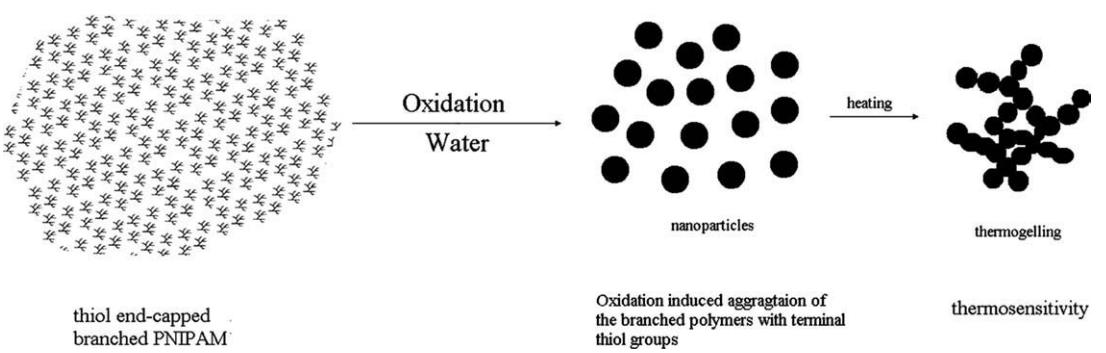

Scheme 2 Oxidative self-association and thermosensitivity of highly branched PNIPAM with thiol end.

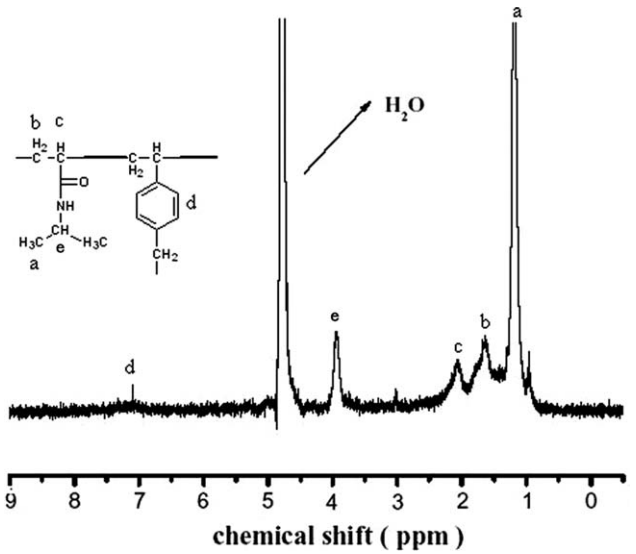

Figure 9 ^{1}H-NMR spectra of the nanoparticle of highly branched PNIPAM HP20 formed at concentration of 1.67% in D_2O.

"solid-like" state and the proton signals in these regions can not be detected due to their smaller relaxation time than the dead time before acquisition.[31]

CONCLUSION

A vinyl contained trithiocarbonate RAFT agent was synthesized and was used as both a controlling radical polymerization chain transfer agent and a monomer to initiate the copolymerization with NIPAM monomer to obtain highly branched PNIPAM. ^{1}H-NMR, DLS, and GPC measurements confirmed the highly branched structure, and the results showed that the degrees of branched depended on the ratio of NIPAM monomer to the RAFT agent. After aminolysis, a multi-thiols capped branched PNIPAM was obtained, which can be crosslinked with each other by the formation of disulfide bonds under oxidant condition. It was found that the branched PNIPAM could be dissolved after a pre-swelling process. Interestingly, DLS and AFM studies revealed that the branched PNIPAM could form nanoparticles through the oxidation induced self-association. A thermogelling behavior has also been found for the nanoparticle system when heating it up to 25°C, and the formed hydrogel showed a thermo-induced collapse when increasing temperature up to 35°C. In addition, a critical size of nanoparticle and a critical gelation concentration were found to the essential criteria for this thermogelling process. A possible mechanism was described, and the thermogelling system has potential application in both nanosciences and biomaterials.

References

1. Mckee, M. G.; Unal, S.; Wilkes, G. L.; Long, T. E. Prog Polym Sci 2005, 30, 507.
2. Magnusson, H.; Malmstro,¨M. E.; Hult, A.; Johansson, M. Polymer 2002, 43, 301.
3. Claesson, H.; Jikei, M.; Kakimoto, M. Prog Polym Sci 2001, 26, 1233.
4. Unger, F.; Wittmar, M.; Morell, F.; Kissel, T. Biomaterials 2008, 29, 2007.
5. Weight, S.; Busse, C.; Bombis, C.; Knudsen, M. M.; Gothelf, K. V.; Laegsgaard, E.; Besenbacher, F.; Linderoth, T. R. Angew Chem Int Ed 2008, 47, 4406.
6. Chi, Y. G.; Scroggins, S. T.; Frechet, J. M. J. J Am Chem Soc 2008, 130, 6322.
7. Bannister, I.; Billingham, N. C.; Arms, S. P.; Rannard, S. P.; Findlay, P. Macromolexules 2006, 39, 7483.
8. Isaure, F.; Cormack, P. A. G.; Sherrington, D. C. Macromolecules 2004, 37, 2096.
9. Vo, C. D.; Rosselgong, J.; Armes, S. P.; You, Y. Z.; Zhou, Q. H.; Manickam, D. S.; Wan, L.; Mao, G. Z.; Oupicky, D. Macromolecules 2007, 40, 7119.
10. Tsarevsky, N. V.; Matyjaszewski, K. Macromolecules 2005, 38, 3087.
11. Sato, T.; Arima, Y.; Seno, M.; Hirano, T. Macromolecules 2005, 38, 1627.
12. Carter, S.; Hunt, B.; Rimmer, S. Macromolecules 2005, 38, 4595
13. Carter, S.; England, R. M.; Hunt, B. L.; Rimmer, S. Macromol Biosci 2007, 7, 975
14. Carter, S.; Rimmer, S.; Rutkaite, R.; Swanson, L.; Fairclough, J. P. A.; Sturdy, A.; Webb, M. Biomacromolecules 2006, 7, 1124.
15. Oudshoorn, M. H. M.; Penterman, R.; Rissmann, R.; Bouwstra, J. A.; Broer, D. J.; Hennink, W. E. Langmuir 2007, 23, 11819
16. Kitamura, T.; Matsumoto, A. Macromolecules 2007, 40, 509.
17. Oudshoorn, M. H. M.; Rissmann, R.; Bouwstra, J. A.; Hennink, W. E. Biomaterials 2006, 27, 5471.
18. Hu, Z. B.; Xia, X. H.; Benee, L. S.; Snowden, M. J.; Chowdhry, B. Z. Adv Mater 2004, 16, 305.
19. Yang, Z. G.; Ding, J. D. Macromol Rapid Commun 2008, 29, 751.
20. Zheng, Q.; Pan, C. Y. Eur Polym J 2006, 42, 807.
21. Bae, S. J.; Suh, J. M.; Sohn, Y. S.; Bae, Y. H.; Kim, S. W.; Jeong, B. Macromolecules 2005, 38, 5260.
22. Zhang, G. Z.; Winnik, F. M.; Wu, C. Phys Rev Lett 2003, 90, 035506
23. Xia, Y.; Burke, N. A. D.; Stolver, H. D. H. Macromolecules 2006, 39, 2275.
24. Li, A.; Lu, Z.; Zhou, Q.; Qiu, F.; Yang, Y. Polymer 2006, 47, 1774.
25. Jikei, M.; Kakimoto, M.; Liu, B. L.; Kazlauciunas, A.; Guthrie, J. T.; Perrier, S. Prog Polym Sci 2001, 26, 1233.
26. Xia, Y.; Yin, X. C.; Burke, N. A. D.; Stolver, H. D. H. Macromolecules 2005, 38, 5937.
27. Whittaker, M. R.; Goh, Y. K.; Gemici, H.; Legge, T. M.; Perrier, S.; Monteiro, J.; Qiu, X. P.; Winnik, F. M. Macromolecules 2006, 39, 9028.
28. Jiang, X.; Liu, S. Y.; Narain, R. Langmuir 2009, 25, 13344.
29. Saito, G.; Swanson, J. A.; Lee, K. D.; Shu, X. Z.; Liu, Y. C.; Luo, Y.; Roberts, M. C.; Prestwich, G. D. Adv Drug Deliv Rev 2003, 55, 199.
30. Plunkett, K. N.; Berkowski, K. L.; Moore, J. S. Biomacromolecules 2005, 6, 632.
31. Larsson, A.; Kuckling, D.; Schönhoff, M. Colloids Surf A: Physicochem Eng Asp 2001, 190, 185.